

# Experimental Study of Waste Tire Rubber, Wood-Plastic Particles and Shale Ceramsite on the Performance of Self-Compacting Concrete

Lei Tian, Liuchao Qiu\*, Jingjun Li and Yongsen Yang

College of Water Resources & Civil Engineering, China Agricultural University, Beijing, 100083, China

\*Corresponding Author: Liuchao Qiu. Email: qiliuchao@cau.edu.cn

Received: 27 September 2019; Accepted: 31 October 2019

**Abstract:** In recent decades, the utilization of waste tires, plastic and artificial shale ceramsite as alternative fine aggregate to make self-compacting concrete (SCC) has been recognized as an eco-friendly and sustainable method to manufacture renewable construction materials. In this study, three kinds of recycled aggregates: recycled tire rubber particles, wood-plastic particles, artificial shale ceramsite were used to replace the sand by different volume (5%, 10%, 20% and 30%), and their effects on the fresh and hardened properties of SCC were investigated. The slump flow and V-funnel tests were conducted to evaluate the fresh properties of modified-SCC mixtures. The hardened properties include 3, 7 and 28-day compressive strengths, axial compressive strength, static elastic modulus, and compressive stress-strain behavior at 28 days. The test results showed that the incorporation of these three kinds of alternative aggregates had a negative impact on the fresh properties of SCC. Besides, the 28-day compressive strength and axial compressive strength decreased with the increase of rubber and wood-plastic particles content. In this experiment, all the three kinds of recycled aggregates can improve the ductility and deformability of SCC, and the most excellent performance comes from SCC with recycled rubber particles.

**Keywords:** Self-compacting concrete; recycled aggregates; lightweight aggregates; waste management

## 1 Introduction

With the development of urbanization and industrialization worldwide, large amounts of solid wastes have been produced. However, open-air accumulation, incineration, and landfill are three common ways to dispose solid wastes [1]. For example, more than 50% of the 100 million tons waste tires in the world were discarded or buried annually without any treatment, and 38% of the 25 million tons of plastic wastes produced annually in the EU were buried [2-3]. These treatments not only cause a quantity of energy and resource consumption, but pollute the environment, posing threaten to human health. Therefore, attention has been focused on recycling waste and promoting sustainable use of resources many years.

Concrete, one of the most widely used building material, plays a significant role during the construction process, and the demand multiplied rapidly. According to statistics, an average of nearly 500 million tons of



This work is licensed under a Creative Commons Attribution 4.0 International License, which permits unrestricted use, distribution, and reproduction in any medium, provided the original work is properly cited.

concrete is consumed yearly [4]. Furthermore, SCC has been rapidly applied worldwide for many years owing to its excellent performance of superb fluidity and segregation resistance [5]. Although SCC has obvious advantages over conventional concrete, the high brittleness and low strain performance of SCC limit its application in some special fields. Adding solid wastes, such as waste tire rubber and plastic, can not only improve the ductility and deformability of SCC [6, 7], but conform to the concept of sustainable development.

Many researches have indicated that the incorporation of waste tires has a certain impact on the self-compacting ability and mechanical properties of SCC. The incorporation of rubber particles can reduce the flow ability and passing ability of SCC [8, 9], making the concrete mixture easily to segregate [10]. The phenomenon is attributed to the rough surface of crumb rubber particles [11], which makes the flow of concrete mixture need to overcome greater internal friction, and the addition of rubber particles also increases the volume of air in SCC [12]. Besides, researches have shown that the incorporation of rubber particles will reduce the splitting tensile strength, compressive strength and elastic modulus of SCC [13, 14]. However, the addition of crumb rubber can improve the ductility [15], toughness [16, 17], impact resistance [18, 19], freeze-thaw resistance [20] and strain performance [21, 22] of concrete. For waste plastic, some scholars have studied the effect of using it as alternative fine aggregate into SCC on self-compacting ability and mechanical properties [23, 24]. Faraj et al. [7] found that with the increase of PP (Polypropylene) plastic particles content, the splitting tensile strength, flexural strength, compressive strength and elastic modulus of SCC decreased, and the ductility increased. Wiswamitra et al. [25] investigated the effect of PET (Polyethylen Terephthalate) wastes on the fresh and mechanical properties of SCC through experiments, and found that when the plastic content was less than 10%, the self-compacting ability of SCC was enhanced with the increase of content, but the tensile strength, compressive strength and elastic modulus were decreased with the content increased. In addition, a new environment - friendly material consisting of plastic and plant fibers has been developed in recent years, which is called wood-plastic composite material and has good strength properties, plasticity and durability [26]. However, there are few studies about the influence of wood-plastic particles on the performance of SCC. In addition, artificial shale ceramsite is also widely used to replace natural aggregates in conventional concrete to improve the performance of concrete, but there are few studies on the replacement of fine aggregate in SCC with artificial shale ceramsite and its effect on the fresh and mechanical characteristics. Bogas et al. [27] investigated the effect of expanded clay aggregates on fresh and mechanical characteristics of SCC and found that the SCC with lightweight aggregates had a slight increase in elastic modulus and a slight decrease in flow properties, but the deformation ability was improved.

In this study, we investigated the fresh and hardened properties of SCC in the case of partial replacement of fine aggregate with recycled tire rubber particles, wood-plastic particles, artificial shale ceramsite respectively, and their effects on the results of slump flow and V-funnel tests, 3, 7 and 28-day compressive strengths, 28-day axial compressive strength, static elastic modulus, and compressive stress-strain behavior have been analyzed and compared.

## 2 Research Significance

Although studies have analyzed most of the properties of SCC mixed with waste tire rubber, plastic and shale ceramsite, there is no comparative study on the performance of SCC mixed with waste tire rubber particles, wood-plastic particles and shale ceramsite. In this paper, the recycled tire rubber particles, wood-plastic particles and artificial shale ceramsite were used as fine aggregate to replace natural sand by different volume, which provides a reference method for improving the ductility and strain performance of traditional SCC.

The use of solid wastes as artificial aggregates to produce SCC is a promising way to reduce the pollution caused by waste tires and plastic to the atmosphere, soil and water sources, and release the exploitation of natural resources. Moreover, the cost of waste disposal into aggregates for the production of SCC is lower than the cost of landfill disposal and natural sand mining. Finally, the incorporation of solid wastes can improve the ductility and strain performance of SCC.

### 3 Materials and Methods

#### 3.1 Materials

##### 3.1.1 Powder Materials

The powder materials used in this test include ordinary Portland cement (C-P.042.5) and Grade I fly ash (FA). In accordance with the Chinese standard GB175 [28], the cement particles are 300 meshes and the apparent density is 3100 kg/m<sup>3</sup>. Grade I fly ash particles, which with an apparent density of 2200 kg/m<sup>3</sup>, are of similar size to cement particles.

##### 3.1.2 Natural Aggregates

In this test, the coarse aggregates are natural gravel (G) with a granule size of 5-20 mm, and the apparent density is 2710 kg/m<sup>3</sup>. The fine aggregate is natural sand (S) of Zone II with a fineness modulus of 2.9, and the apparent density is 2670 kg/m<sup>3</sup>. The sampling and testing methods of aggregates are based on the Chinese standard SL 352 [29]. The grading curves and photograph photos are shown in Figs. 1 and 2.

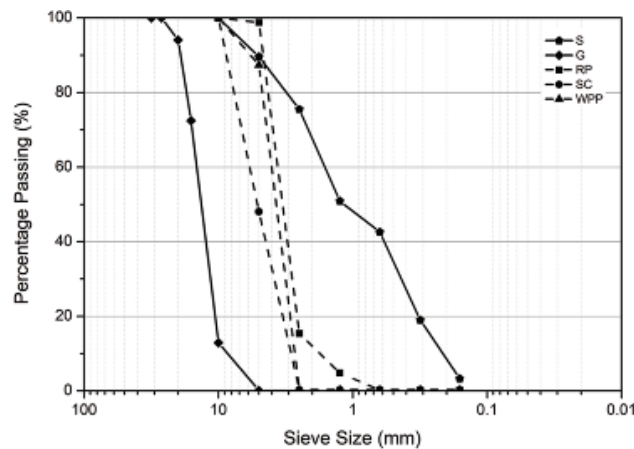


Figure 1: Sieve analysis of rubber particles, shale ceramsite, wood-plastic particles, fine and coarse aggregates

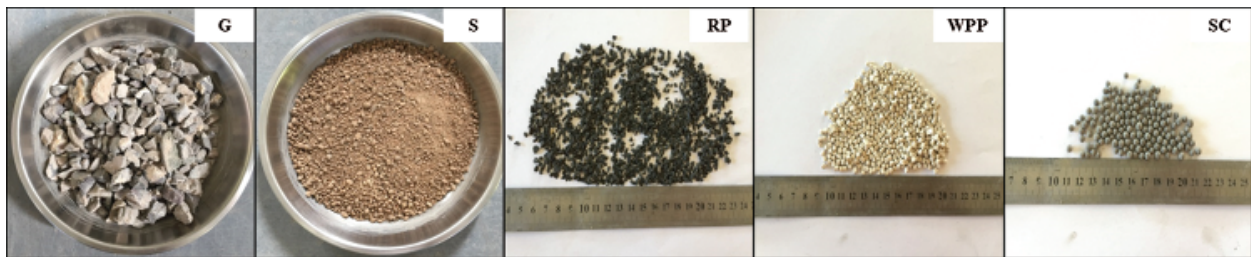


Figure 2: Photograph photos of gravel, sand, rubber particles, wood-plastic particles, and shale ceramsite

### 3.1.3 Rubber Particles

The granule size of rubber particles (RP) used in this test is 2-4 mm, which is obtained from the crushing of waste tires. The packing density and apparent density are  $710 \text{ kg/m}^3$  and  $1600 \text{ kg/m}^3$ , respectively. The grading curves and photograph photos are shown in Figs. 1 and 2.

### 3.1.4 Wood-Plastic Particles

The wood-plastic particles (WPP) used in this test are a kind of new composite material composed of recycled polypropylene plastic (PP) and straw, which have good durability and certain elasticity. WPP used in this test is cylindrical granules with a diameter of 2 mm and a height of 2-4 mm. The packing density and apparent density are  $625 \text{ kg/m}^3$  and  $1040 \text{ kg/m}^3$ , respectively. The water absorption rates at 1 h and 24 h are 2.0% and 5.0%, respectively. The grading curves and photograph photos are shown in Figs. 1 and 2.

### 3.1.5 Shale Ceramsite

The shale ceramsite (SC) used in this test is spherical granules with a diameter of 2-4 mm. The packing density and apparent density are  $980 \text{ kg/m}^3$  and  $1980 \text{ kg/m}^3$  respectively, and the tube strength is 4 MPa. The porosity is 33%, and the water absorption rates at 1 h and 24 h are 12.0% and 14.3%, respectively. The grading curves and photograph photos are shown in Figs. 1 and 2.

### 3.1.6 Chemical Admixture

The chemical admixture used in this test is a kind of high-range water reducer (HRWR) with a solid content of 20%. The rheological properties of SCC were adjusted by changing the dosage of HRWR in this test, so that SCC has a good fluidity and segregation resistance.

## 3.2 Mix Proportions

Throughout the experimental study, the total amount of powder materials was  $498 \text{ kg/m}^3$ , and the water-powder ratio by volume was 0.95, which remained constant. The total volume of powder materials contained 52.0% cement and 48.0% fly ash, and the sand to aggregates ratio by volume was 44.0%.

In this study, three series of SCC mixtures were designed, and three different kinds of granular materials were used to replace the fine aggregate at incremental volume percentages of 5%, 10%, 20% and 30%, respectively. A total of thirteen SCC mix proportions are given in Tab. 1. The Mix ID SCRC-5, SCSC-5, SCWC-5 and CS denote the mixtures with RP replaced at 5% by volume, the mixture with SC replaced at 5% by volume, the mixture with WPP replaced at 5% by volume and control group SCC, respectively.

## 3.3 Preparation of Alternative Aggregates

The RP, SC and WPP were sieved to remove impurities prior to be used. In addition, the SC was immersed in water for 1 hour before being used, and then taken out to a saturated surface dry condition for mixing [30, 31].

## 3.4 Sampling and Curing

In order to test the hardened properties of SCC, nine  $100 \times 100 \times 100$  mm cube concrete specimens and six  $150 \times 150 \times 300$  mm concrete specimens were prepared for each mix proportion. The former were used to test the compressive strengths ( $f_{cu}$ ) of 3, 7 and 28 days, and the latter were used to test the axial compressive strength ( $f_c$ ), static elastic modulus ( $ME$ ) and compressive stress-strain behavior. The SCC was not vibrated during the whole pouring process, and the specimens with molds were then covered with plastic film to prevent evaporation of water. The test specimens were demolded after being cured in the environment of  $20 \pm 2^\circ\text{C}$  for 24 h, and then the demolded specimens were cured to the testing ages in standard curing conditions with a temperature of  $20 \pm 2^\circ\text{C}$  and a humidity of 95%.

**Table 1:** Mix proportions of SCC mixtures

Mix ID	Mix proportions (kg/m <sup>3</sup> )									Demold density (kg/m <sup>3</sup> )
	W/P	S/A	C	FA	G	S	AA	W	SP	
CS	0.95	44%	324	174	762	866	0	186	6.25	2376
SCRC-5	0.95	44%	324	174	762	823	26	186	7.25	2357
SCRC-10	0.95	44%	324	174	762	779	52	186	7.25	2335
SCRC-20	0.95	44%	324	174	762	693	104	186	7.25	2302
SCRC-30	0.95	44%	324	174	762	606	156	186	6.50	2257
SCSC-5	0.95	44%	324	174	762	823	32	186	7.50	2379
SCSC-10	0.95	44%	324	174	762	794	64	186	7.50	2371
SCSC-20	0.95	44%	324	174	762	693	128	186	7.50	2356
SCSC-30	0.95	44%	324	174	762	606	193	186	6.10	2328
SCWC-5	0.95	44%	324	174	762	823	17	186	7.50	2384
SCWC-10	0.95	44%	324	174	762	779	34	186	7.00	2366
SCWC-20	0.95	44%	324	174	762	693	67	186	7.50	2300
SCWC-30	0.95	44%	324	174	762	606	101	186	6.25	2250

**Note:** W/P = Water-Power ratio by volume; S/A = Sand-Aggregate ratio by volume; AA = Alternative Aggregate; W = Water; SP = Super plasticizer.

### 3.5 Sample's Test Methods

In this test, the compressive strength, static elastic modulus and stress-strain behavior of the hardened concrete were examined. In the compressive strength tests, three 100 × 100 × 100 mm cube specimens were tested at 3, 7 and 28 days, respectively. The loading process followed the Chinese standard SL 352 [29], and the loading speed was controlled at 3-5 KN/s.

Furthermore, in accordance with the Chinese standard SL 352 [29], the axial compressive strength and static elastic modulus of concrete were tested using three 150 × 150 × 300 mm concrete specimens, respectively. The compressive stress-strain behavior of the concrete was tested finally. The details of the test process are shown in Fig. 3.

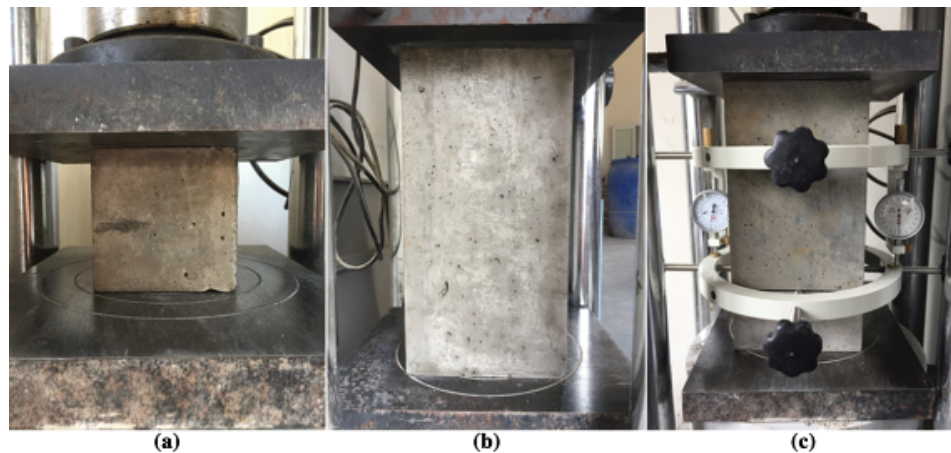


**Figure 3:** Test details of (a) compressive test setup, (b) axis compressive test setup, and (c) static elastic modulus test setup



### 3.6 Fresh Properties

The self-compacting ability follows the Chinese standard JGJ/T283, as shown in Tab. 2 [32]. In this test series, the fluidity, filling ability and viscosity of the fresh SCC were evaluated by the slump flow and V-funnel tests, and the spreading diameter ( $SF$ ), slump height ( $Sh$ ) and V-funnel time ( $t_{V\text{-funnel}}$ ) were measured. The details of slump flow and V-funnel tests are shown in Figs. 4 and 5.

**Table 2:** Self-compacting ability and requirements of SCC

Characteristic	Test method	Measured value	Class	Performance index
flowability	slump-flow test	spreading diameter	$SF1$	550 - 650 mm
			$SF2$	660 - 750 mm
			$SF3$	760 - 850 mm
viscosity	V-funnel test	time	$VF1$	$\leq 8$ s
			$VF2$	9 - 25 s



**Figure 4:** Slump flow test



**Figure 5:** V-funnel test

## 4 Results and Discussion

### 4.1 Fresh Properties

The results of slump flow and V-funnel tests of fresh concrete are shown in Tab. 3, Figs. 6, and 7. The test results show that replacing the fine aggregate with RP, WPP, SC has a negative effect on the rheological properties of SCC. As the RP content increases, the *SF* of concrete gradually decreases, and the  $t_{V\text{-funnel}}$  gradually increases. This is because the RP has a rough surface and the movement of rubber particles requires more energy to overcome the friction resistance between particles [33]. Compared with irregularly shaped RP, the replacement of fine aggregate with spherical SC by volume has a relatively small effect on the fluidity of concrete mixtures, which is attributed to the fact that the SC used in the test is spherical, and the friction resistance between particles to be overcome during the flow is small, and the paste is more likely to flow with SC together [34]. In addition, it was observed that when the fine aggregate was replaced by the same volume of WPP, the particle showed a significant upward movement tendency during the flow of concrete mixtures due to the small density of WPP. When the content of WPP was more than 10%, the phenomenon of particle floating upward was serious, which made the concrete mixtures to easily block the V-funnel, resulting in an increase in  $t_{V\text{-funnel}}$ .

**Table 3:** Fresh properties of tested concrete mixtures

Mix ID	Workability		
	Slump flow (mm)	Slump height (mm)	V-funnel time (s)
CS	735	275	9.66
SCRC-5	725	270	10.15
SCRC-10	720	275	16.87
SCRC-20	650	260	18.63
SCRC-30	645	265	73.56
SCSC-5	700	270	12.41
SCSC-10	715	270	17.35
SCSC-20	655	265	21.75
SCSC-30	665	270	63.4
SCWC-5	665	270	16.38
SCWC-10	625	275	20.06
SCWC-20	645	275	44.22
SCWC-30	585	260	55.19

Based on the results, it can be found that when the content of RP, SC and WPP is more than 10%, the self-compacting ability and segregation resistance of concrete mixtures are greatly reduced. This is because the size of alternative aggregates used in the test is all distributed at 2-4 mm. When the content of alternative aggregates increases to more than 10%, the proportion of fine aggregate in concrete distributed between 2-4 mm increases remarkably, which causes the continuous gradation of fine aggregate to be destroyed and the “interlock effect” between coarse aggregates, so that it greatly reduces the self-compacting ability and segregation resistance of SCC [35]. In addition, since the apparent density of RP and WPP is much lower than that of natural sand, and the bond strength between particles and cement matrix is weak, which make the RP and WPP have an upward movement tendency, making the SCC easier to segregate [21, 27].

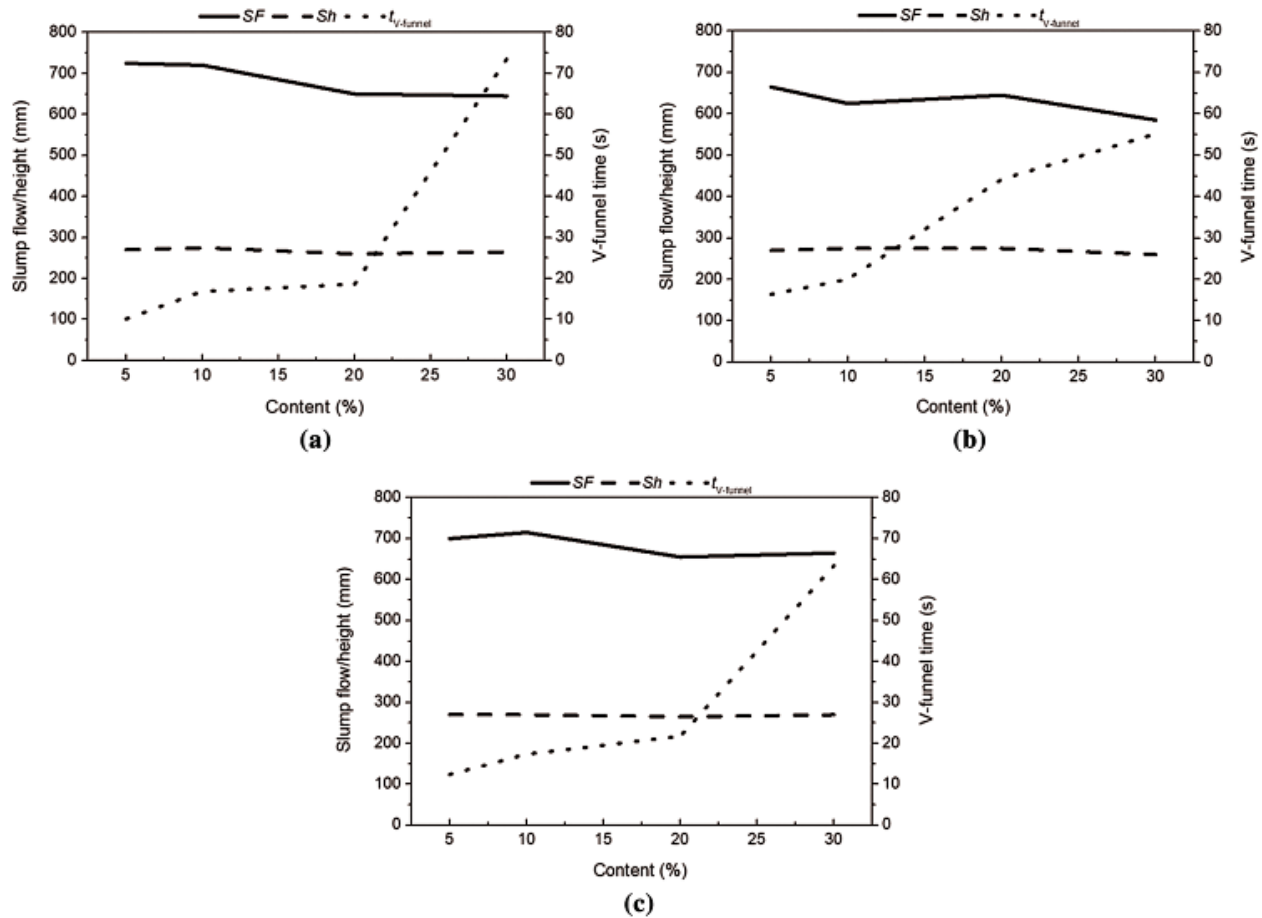


**Figure 6:** Slump flow, Slump height and V-funnel time of (a) SCRC, (b) SCWC, and (c) SCSC

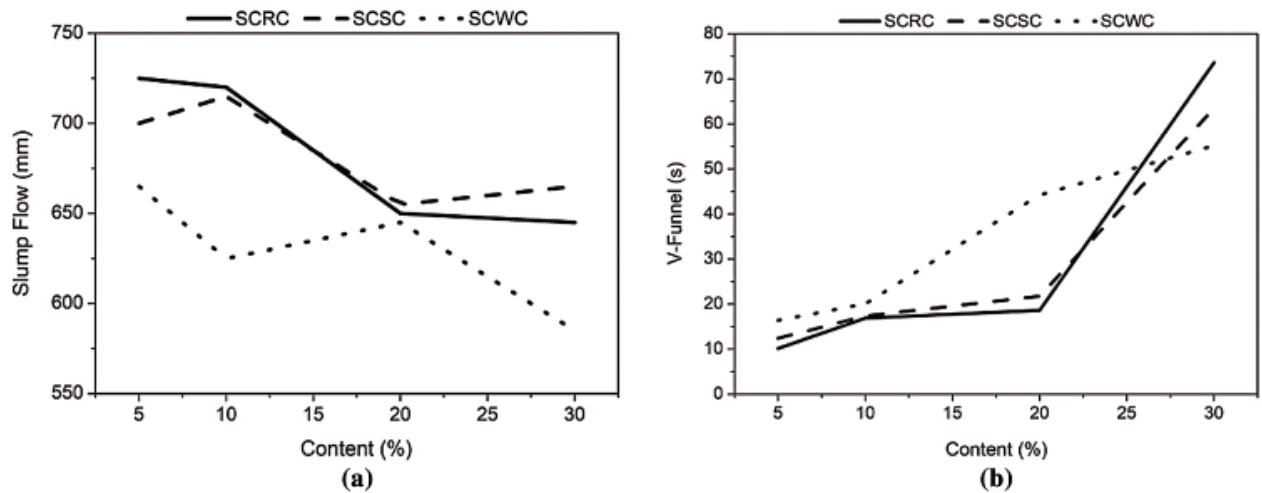


**Figure 7:** Comparison of (a) Slump flow, and (b) V-funnel time of SCRC, SCSC and SCWC



From Tab. 3, Figs. 6 and 7, it is found that the control group SCC obtains the largest  $SF$  of 735 mm and the shortest  $t_{V\text{-funnel}}$  of 9.66 s, and there is no segregation. Compared with the other two series of concrete mixtures, when the content of RP is 5% and 10%, a larger  $SF$  is obtained; when the content is 20% and 30%, the  $SF$  is similar to the other two series. In addition, as the RP content increases, the  $t_{V\text{-funnel}}$  increases gradually, but when the contents of three alternative aggregates are the same, the  $t_{V\text{-funnel}}$  of the SCRC is shorter than the other two concrete mixtures. This is because the other two kinds of alternative materials have a higher water absorption compared with RP. During the flow of concrete mixtures, the free water content was reduced, resulting in the increase of plastic viscosity and  $t_{V\text{-funnel}}$  of concrete mixtures [36]. Although the fluidity and viscosity of SCC decrease with the increase of RP and SC content, when the content doesn't exceed 20%, the  $SF$  and  $t_{V\text{-funnel}}$  are between  $SF1$ ,  $SF2$  and  $VF2$  respectively, which meet the requirements of Chinese standard JGJ/T283 [32]. When the content of RP, SC and WPP are more than 20%, although the  $SF$  can meet the requirements of  $SF1$  and  $SF2$ , the concrete segregation occurs due to the destruction of continuous gradation of the fine aggregate in concrete, which makes the concrete mixture blocked in V-funnel test, and the  $t_{V\text{-funnel}}$  increases.

The distribution of alternative aggregates for all three test series is presented in Fig. 8. It was observed that the distribution of alternative aggregates in three series of concrete mixtures was relatively uniform and there was no obvious stratification. This was because the amount of HRWR was appropriate during the concrete mixing process [21].

## 4.2 Hardened Properties

### 4.2.1 Compressive Strength

The 3, 7 and 28 days compressive strength test results of all concrete mixtures are shown in Tab. 4 and Fig. 9. It is found that the 28-day compressive strength of SCRC gradually decreases with the increases of RP content, which is consistent with the conclusions obtained in the prior research [37]. Due to the low bond strength between RP and cement matrix, it is easy to form a relatively weak interface transition zone (ITZ), which causes a lot of tiny voids and cracks in the ITZ regions. During the compression of SCRC, the ITZ area is the first to be destroyed, and the more RP content, the more compressive strength decreases [8, 12, 21]. Under the same content of alternative aggregates, the 28-day compressive strength of SCWC is higher than that of SCRC, which is attributed to the fact that the compressive strength of WPP is larger than that of RP, and the difference of deformation amount between WPP and cement matrix is small during the compression process. WPP is a kind of composite material composed of PP plastic and straw. Its strength is lower than that of the surrounding cement matrix, and the ITZ area between particles and concrete is weak. Therefore, as the content of WPP increases, the amount of ITZ increases, and the 28-day compressive strength of SCWC decreases [38].

At the same content, the 28-day compressive strength of SCSC (43.7-39.7 MPa) is higher than that of the other two test series. This is because the main component of SC is  $\text{SiO}_2$ , which makes the bond strength between SC and cement matrix higher. In addition, since the SC is spherical, the good flow state of fresh concrete mixtures contributes to the elimination of air, resulting in fewer voids and cracks in the ITZ area [39]. Furthermore, since the SC has relatively high compressive strength and it is immersed in water for 1 h before being used, the water absorbed by SC provides conditions for further hydration of cement inside the concrete during the curing process of SCSC [40]. Compared with the existing studies on replacing coarse aggregates with SC, the method of replacing fine aggregate with SC partially in this test has little effect on the compressive strength of SCC, which is attributed to the coarse aggregates accounts for a large proportion of concrete and plays a major role in controlling the compressive strength of concrete [21]. It could be found in Fig. 10 that the failure surface of SCSC was destroyed along a part of SC fracture, but the SCRC and the SCWC were destroyed along the bonding interface of granules and cement matrix. Therefore, the addition of SC had little negative effect on the compressive strength of

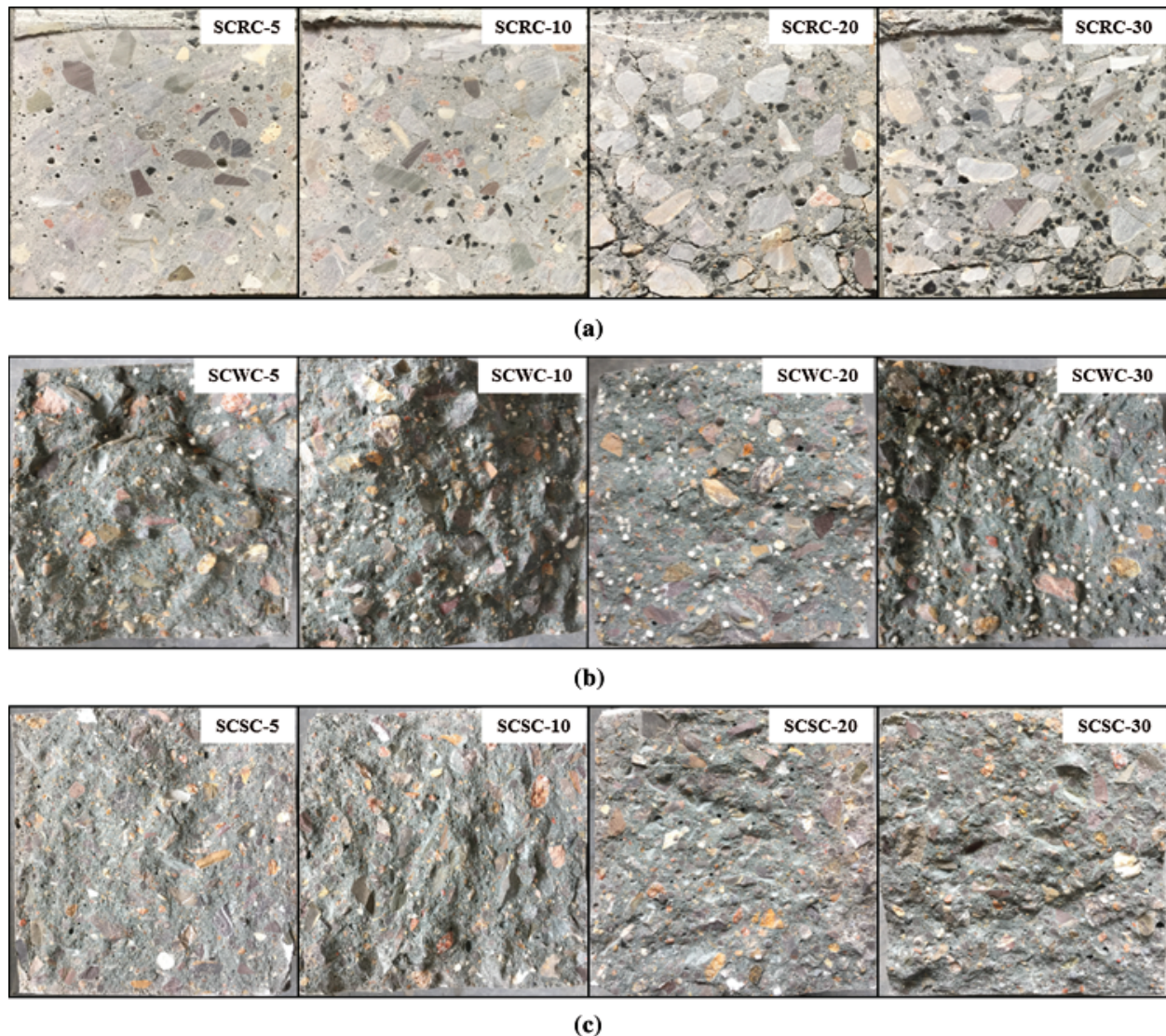


**Figure 8:** Aggregate distribution of (a) SCRC, (b) SCWC, and (c) SCSC

SCC, and the 28-day compressive strength of SCSC was higher than that of SCRC and SCWC under the same volume of alternative aggregates.

It could be seen from Fig. 10 that when the content of the three kinds of granular materials was high and the concrete specimens were compressed to damage, the SCRC had good ductility and compressibility, and the concrete specimens were relatively intact after being destructed. When SCSC and SCWC were destroyed under pressure, the surface mortar and part of the coarse aggregates peeled off. The concrete exhibited weak ductility and strong brittleness compared with SCRC.

#### 4.2.2 Axial Compressive Strength

The response characteristics of 28-day axial compressive strength of concrete mixtures with different amount of alternative aggregate are similar to the 28-day standard compressive strength, as shown in Fig. 11. Compared with the control group SCC, the axial compressive strength decreases gradually with

**Table 4:** Hardened properties of tested concrete mixtures

Mix ID	$f_{cu}$ (MPa)			$f_c$ (MPa)	$ME$ (GPa)
	3-day	7-day	28-day	28-day	28-day
CS	20.5	28.1	44.0	36.7	34.2
SCRC5	20.2	28.0	41.4	35.7	33.1
SCRC10	18.8	27.7	36.7	32.0	29.7
SCRC20	17.4	23.0	32.7	30.1	26.7
SCRC30	13.1	16.0	22.3	22.5	23.6
SCSC5	25.7	34.1	42.3	35.8	36.3
SCSC10	22.3	24.5	39.7	31.5	36.2
SCSC20	22.4	32.6	41.3	35.1	35.4
SCSC30	21.1	28.9	43.7	34.6	33.1
SCWC5	21.8	27.1	42.2	37.8	39.4
SCWC10	22.7	28.4	39.3	35.9	41.0
SCWC20	23.6	32.4	39.0	32.3	39.8
SCWC30	19.5	23.0	34.4	27.4	33.2

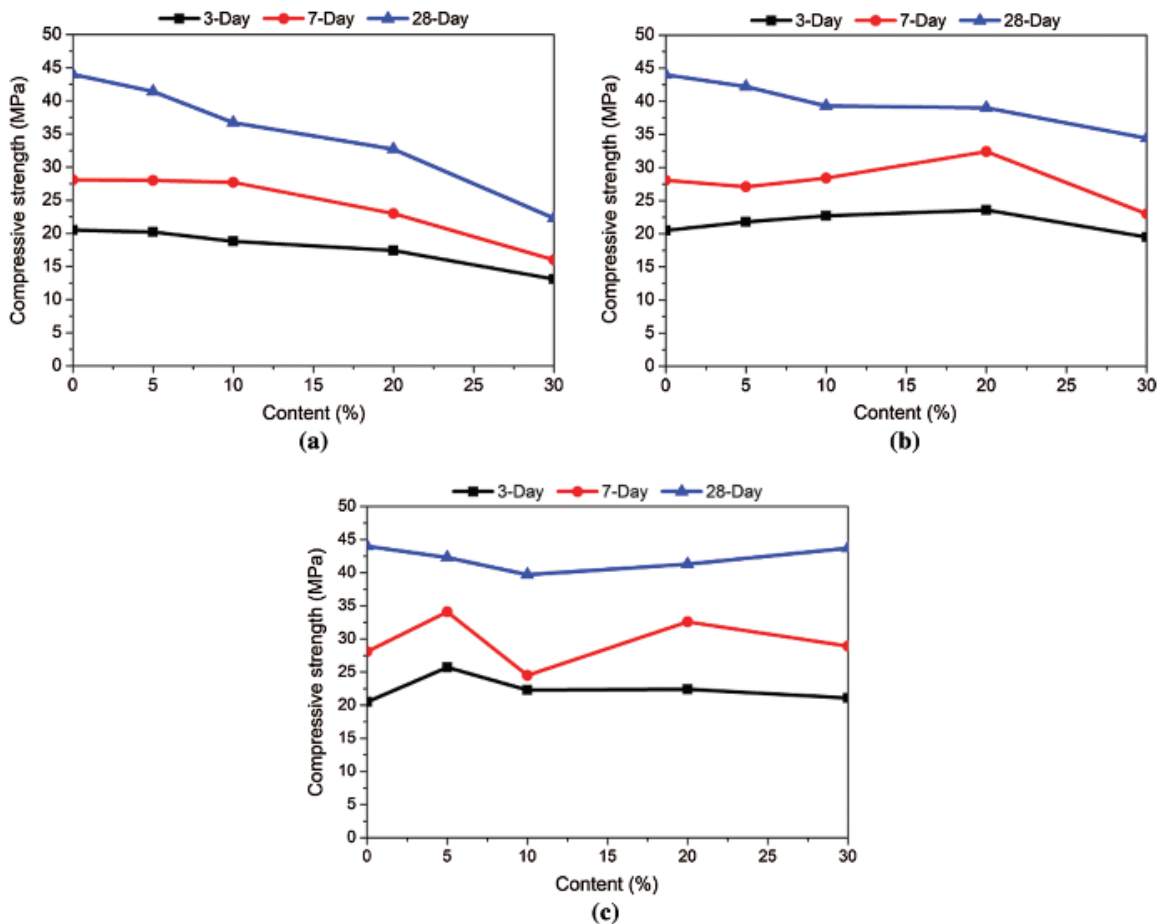


**Figure 9:** 3, 7, & 28 days compressive strength results of (a) SCRC, (b) SCWC, and (c) SCSC series



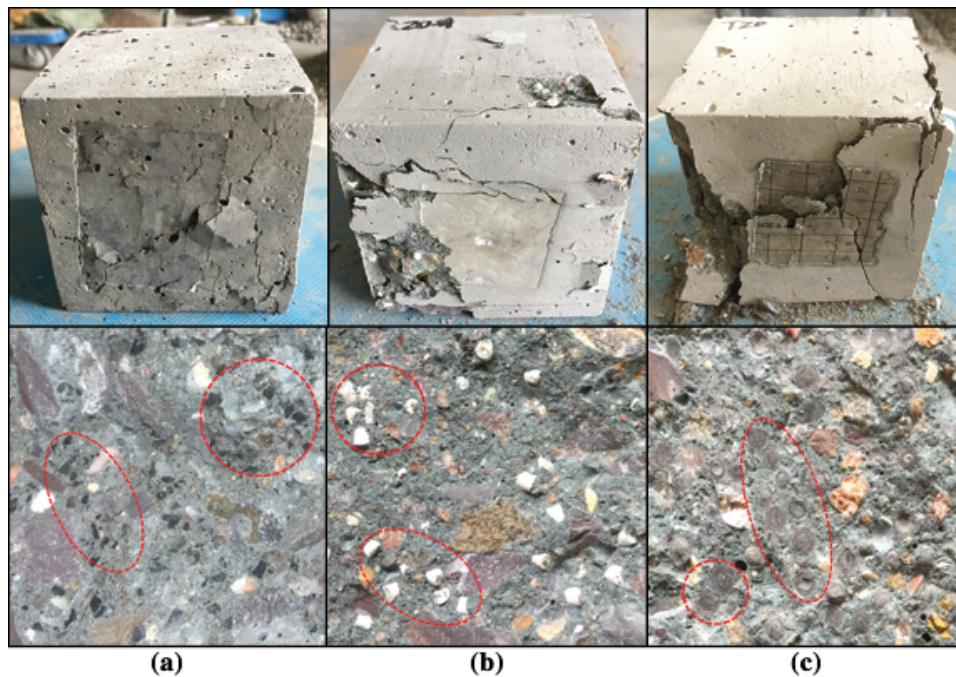


**Figure 10:** Failure modes and failure interfaces of (a) SCRC, (b) SCWC, and (c) SCSC

the RP content increases. When the RP content is 5%, 10%, and 20%, the axial compressive strength of concrete mixtures decreases by 2.7%, 12.8%, and 18.0%, respectively; when the RP content is 30%, the compressive strength decreases greatly, down by 38.7%. The axial compressive strength of SCWC shows a tendency to increase first and then decrease with the increase of WPP content. When the content is 5%, the axial compressive strength is increased by 3.0%, and at 10%, 20%, and 30%, the axial compressive strength decreases by 2.2%, 12.0%, and 25.3%, respectively. When the content of RP and WPP is more than 20%, the axial compressive strength of concrete is decreased greatly, which is attributed to the weak bond between alternative aggregates and surrounding cement matrix. And with the increases of content, the continuous gradation of fine aggregate is destroyed, which leads to a significant increase in pore

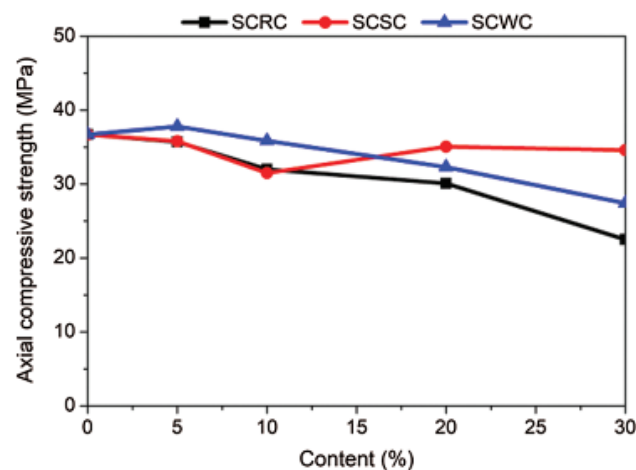


**Figure 11:** Axial compressive strength results of SCRC, SCSC, and SCWC series

volume and ITZ in the concrete and a significant decrease in axis compressive strength [12]. Compared with SCRC and SCWC, the axial compressive strength of SCSC decreases less because the main components of SC being used in the test is similar to the sand and the difference in density is small, which makes the bond strength between SC and cement matrix is relatively high. Besides, the water absorbed in the pores of SC will be released into the surrounding cement paste during the curing of SCSC to promote the internal curing of the surrounding concrete [40].

#### 4.2.3 Static Elastic Modulus

Fig. 12 shows the test results of static elastic modulus of concrete mixtures. It can be found that when the RP content is 5%, 10%, 20% and 30%, the static elastic modulus of SCRC decreases by 3.2%, 13.2%, 21.9%, and 31.0% respectively compared with the control group SCC. The causes of this phenomenon can be summarized as: voids in the weak area of ITZ between RP and cement matrix, the difference in strain performance between RP and cement matrix results in higher internal stresses in the concrete perpendicular to the load direction, the compressive strength depends mainly on the properties of coarse aggregates and the RP has better deformation performance than concrete [15]. When the SC content is 5%, 10%, 20%, the static elastic modulus of SCSC increases by 6.1%, 5.8%, and 3.5% respectively, and when the content is 30%, the static elastic modulus decreases by 3.2%. When the content of WPP is 5%, 10% and 20%, the static elastic modulus of SCWC increases by 15.2%, 19.9%, and 16.4%, respectively. However, when the content increases to 30%, the elastic modulus decreases by 2.9%. It can be found that the incorporation of RP has a significant effect on the reduction of static elastic modulus of concrete compared with the incorporation of SC and WPP. Therefore, the addition of RP can reduce the brittleness of concrete, enhance the strain ability, and the higher the RP content, the more obvious the effect.

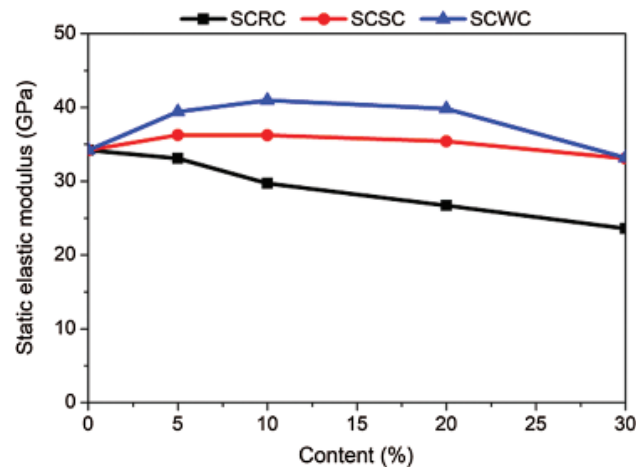


**Figure 12:** Static elastic modulus of SCRC, SCSC, and SCWC series

#### 4.2.4 Compressive Stress-Strain Behavior

The compressive stress-strain relationship is an important properties of concrete, which can predict the behavior of concrete structure under load [41]. Fig. 13 shows the stress-strain curves of SCRC, SCSC, and SCWC test series. For this test, the concrete specimens were compressed and the strain was measured by the concrete elastic modulus meter. The maximum compressive stress was 80% of the axial compressive strength. From the three sets of stress-strain curves, it can be found that when the compressive stress is less than 60% of the axial compressive strength, the concrete specimens are elastically deformed, and



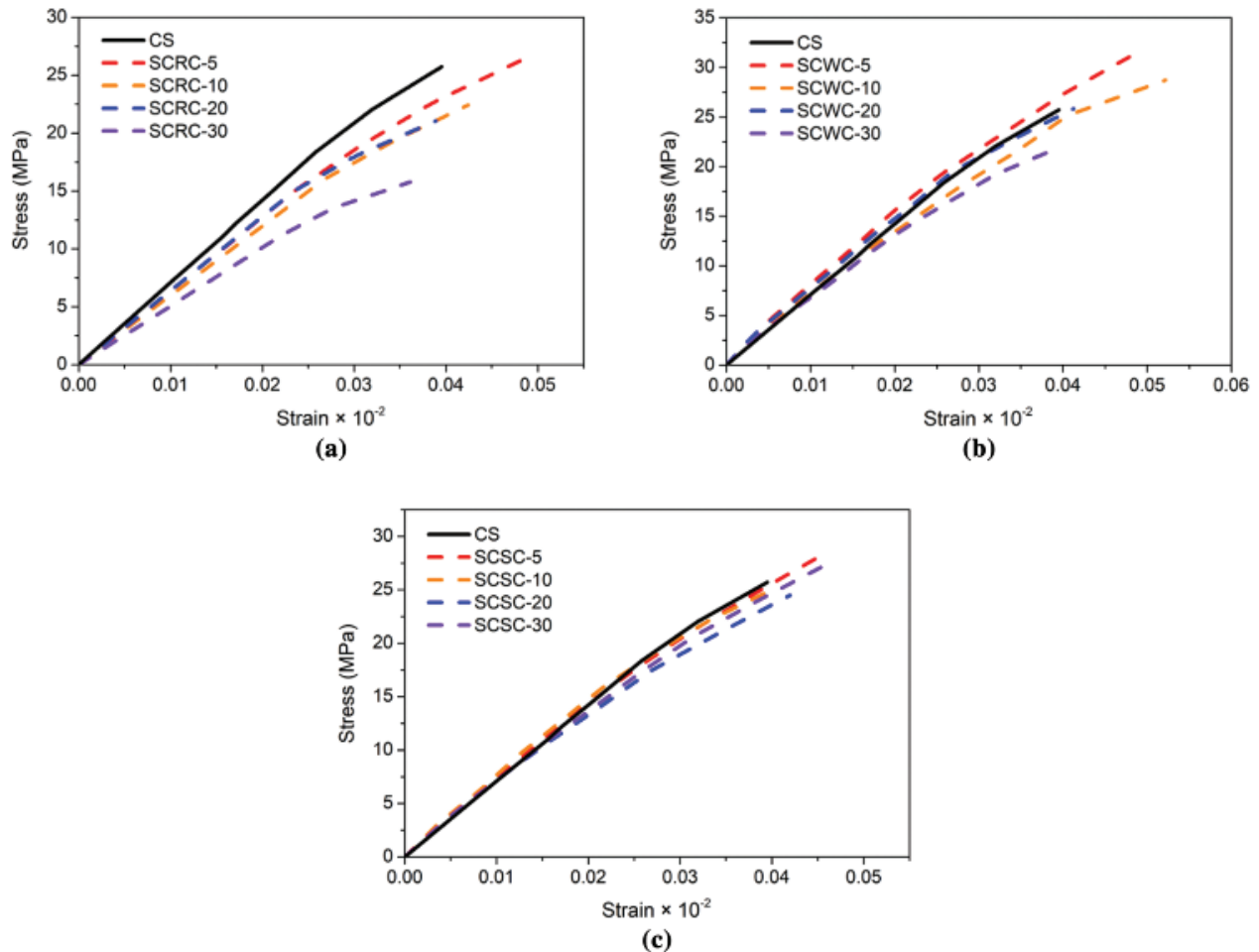


**Figure 13:** Compressive stress-strain curves for (a) SCRC, (b) SCWC, and (c) SCSC series

when it is greater than 60%, the concrete specimens begin to plastically deform. When the plastic deformation begins, the strain is between 0.0002-0.00035. The results also indicate that under the same stress condition, the strain of SCRC increases the most with the increase of alternative aggregate content, which shows that with the increase of RP content, the failure mode of concrete specimen changes from brittle failure to ductile failure.

## 5 The Cost Effectiveness for Applying the Recycled Waste Aggregate

According to a recent market survey by the China Sand and Stone Association, the national average price of natural sand is about \$13.5 per ton, and in the Yangtze River Valley, the cost of sand is up to \$21 per ton [42]. It can directly reduce the cost of concrete by replacing natural sand with tire rubber particles, plastic and shale ceramsite. In addition, replacing natural aggregates with tire rubber particles, plastic and shale ceramsite not only reduces the waste incineration cost and site cost for landfills and dumps, but also saves sand resources, which is beneficial to both society and the ecological environment. In the decade of 2008-2018, average waste incineration cost was at \$9~\$13 per ton [43]. The cost of refuse disposal in Shanghai was close to \$71 per ton in 2013 [44]. Researches had shown that the price of waste tires can be \$57 per ton [45], and the price of waste tires has fallen in recent years [46]. The price of shale ceramsite changed slightly from 2011 to 2017, with an average price of approximately

\$13.5 per ton [47]. The price of recycled plastic can be \$183.6 per ton based on its variety and quality [48]. Meanwhile, the price of traditional concrete aggregates is still growing owing to the continuous reduction of natural sand resources and the high transportation expenses [49]. Furthermore, the total cost of refuse disposal continues to increase with the increasing quantity of solid wastes, and the damage caused by solid wastes to the environment increases gradually, so replacing natural aggregates with solid waste aggregates has a good application prospect.

## 6 Conclusions

Three different lightweight aggregates (recycled RP made from waste tires, WPP made of PP plastic and straw, and shale ceramsite) and their effects on the fresh and hardened properties of SCC have been investigated. The conclusions are as follows:

The self-compacting ability of concrete mixtures decreased with the increase of RP, WPP and SC content. On the other hand, the test group incorporating SC obtained the highest cubic compressive strength (39.7-43.7 MPa) and axial compressive strength (31.5-35.8 MPa) compared with the other two series of concrete mixtures, and the test group incorporating WPP had obtained the highest static elastic modulus (33.2-41.0 GPa). Besides, when the SC content was not less than 5%, the static elastic modulus of SCSC gradually decreased as the content increased, and the 28-day compressive strength of SCWC decreased with the increase of WPP content.

Increasing the RP content from 5% to 30%, the compressive strength and static elastic modulus descended and ranged in 22.3-41.4 MPa and 23.6-33.1 GPa respectively. When the RP content was 5%, 10%, 20% and 30%, the static elastic modulus decreased by 3.22%, 13.16%, 21.93%, and 30.99% respectively, which indicated that the ductility and strain performance of SCRC were improved gradually with the increase of RP content. Furthermore, the failure mode of concrete specimen is changed from brittle failure to ductile failure. When the RP content reached 20% of the total volume of fine aggregate, the SCRC still satisfied the self-compacting ability and the compressive strength can reach 32.7 MPa while static elastic modulus dropped to 26.7 GPa.

Finally, the SCRC exhibits the maximum strain and minimum static elastic modulus in the same alternative aggregate content and stress compared with the other two concrete mixtures, so the best choice among the three materials for improving the ductility and strain performance of SCC is RP.

**Acknowledgement:** The author gratefully acknowledge the financial support from the National Natural Science Foundation of China, grant number 11772351, Double Shield TBM Material Optimization and Supporting Technology Research - TBM Segment Rapid Support Scientific Research Project [contract NO: PM2017/D02] and the National Key R & D Program of China (No. 2018YFC0406604).

**Conflicts of Interest:** The authors declare that they have no conflicts of interest to report regarding the present study.

## References

1. Zhou, H. X., Bhattarai, R., Li, Y. K., Li, S. Y., Fan, Y. H. (2019). Utilization of coal fly and bottom ash pellet for phosphorus adsorption: sustainable management and evaluation. *Resources, Conservation and Recycling*, 149, 372–380. DOI 10.1016/j.resconrec.2019.06.017.
2. Thomas, B. S., Gupta, R. C. (2016). A comprehensive review on the applications of waste tire rubber in cement concrete. *Renewable and Sustainable Energy Reviews*, 54, 1323–1333. DOI 10.1016/j.rser.2015.10.092.
3. Ledererová, M., Štefunková, Z., Gregorová, V., Urbán, D. (2019). The issue of plastic waste in the environment and its possible uses as a substitute for filler in lightweight concrete. *IOP Conference Series: Materials Science and Engineering*, 549, 012032. DOI 10.1088/1757-899X/549/1/012032.

4. Richardson, A. E., Coventry, K. A., Ward, G. (2012). Freeze/thaw protection of concrete with optimum rubber crumb content. *Journal of Cleaner Production*, 23(1), 96–103. DOI 10.1016/j.jclepro.2011.10.013.
5. Aslani, F. (2013). Effects of specimen size and shape on compressive and tensile strengths of self-compacting concrete with or without fibres. *Magazine of Concrete Research*, 65(15), 914–929. DOI 10.1680/macr.13.00016.
6. Zhu, H., Rong, B., Xie, R., Yang, Z. H. (2018). Experimental investigation on the floating of rubber particles of crumb rubber concrete. *Construction and Building Materials*, 164, 644–654. DOI 10.1016/j.conbuildmat.2018.01.001.
7. Faraj, R. H., Sherwani, A. F. H., Daraei, A. (2019). Mechanical, fracture and durability properties of self-compacting high strength concrete containing recycled polypropylene plastic particles. *Journal of Building Engineering*, 25, 100808. DOI 10.1016/j.jobbe.2019.100808.
8. AbdelAleem, B. H., Hassan, A. A. A. (2018). Development of self-consolidating rubberized concrete incorporating silica fume. *Construction and Building Materials*, 161, 389–397. DOI 10.1016/j.conbuildmat.2017.11.146.
9. Aslani, F., Ma, G., Yim Wan, D. L., Muselin, G. (2018). Development of high-performance self-compacting concrete using waste recycled concrete aggregates and rubber granules. *Journal of Cleaner Production*, 182, 553–566. DOI 10.1016/j.jclepro.2018.02.074.
10. Topçu, İ. B., Bilir, T. (2009). Experimental investigation of some fresh and hardened properties of rubberized self-compacting concrete. *Materials & Design*, 30(8), 3056–3065. DOI 10.1016/j.matdes.2008.12.011.
11. Guo, S., Dai, Q., Si, R., Sun, X., Lu, C. (2017). Evaluation of properties and performance of rubber-modified concrete for recycling of waste scrap tire. *Journal of Cleaner Production*, 148, 681–689. DOI 10.1016/j.jclepro.2017.02.046.
12. Li, N., Long, G. C., Ma, C., Fu, Q., Zeng, X. H. et al. (2019). Properties of self-compacting concrete (SCC) with recycled tire rubber aggregate: a comprehensive study. *Journal of Cleaner Production*, 236, 117707. DOI 10.1016/j.jclepro.2019.117707.
13. Ismail, M. K., Hassan, A. A. A. (2016). Use of metakaolin on enhancing the mechanical properties of self-consolidating concrete containing high percentages of crumb rubber. *Journal of Cleaner Production*, 125, 282–295. DOI 10.1016/j.jclepro.2016.03.044.
14. Si, R., Wang, J., Guo, S., Dai, Q., Han, S. (2018). Evaluation of laboratory performance of self-consolidating concrete with recycled tire rubber. *Journal of Cleaner Production*, 180, 823–831. DOI 10.1016/j.jclepro.2018.01.180.
15. Hilal, N. N. (2017). Hardened properties of self-compacting concrete with different crumb rubber size and content. *International Journal of Sustainable Built Environment*, 6(1), 191–206. DOI 10.1016/j.ijbs.2017.03.001.
16. Reda Taha, M. M., El-Dieb, A. S., Abd El-Wahab, M. A., Abdel-Hameed, M. E. (2008). Mechanical, fracture, and microstructural investigations of rubber concrete. *Journal of Materials in Civil Engineering*, 20(10), 640–649. DOI 10.1061/(ASCE)0899-1561(2008)20:10(640).
17. Chen, X. D., Liu, Z. H., Guo, S. S., Huang, Y. B., Xu, W. L. (2019). Experimental study on fatigue properties of normal and rubberized self-compacting concrete under bending. *Construction and Building Materials*, 205, 10–20. DOI 10.1016/j.conbuildmat.2019.01.207.
18. AbdelAleem, B. H., Ismail, M. K., Hassan, A. A. A. (2018). The combined effect of crumb rubber and synthetic fibers on impact resistance of self-consolidating concrete. *Construction and Building Materials*, 162, 816–829. DOI 10.1016/j.conbuildmat.2017.12.077.
19. Khalil, E., Abd-Elmohsen, M., Anwar, A. M. (2019). Impact resistance of rubberized self-compacting concrete. *Water Science*, 29(1), 45–53. DOI 10.1016/j.wsj.2014.12.002.
20. Gonen, T. (2018). Freezing-thawing and impact resistance of concretes containing waste crumb rubbers. *Construction and Building Materials*, 177, 436–442. DOI 10.1016/j.conbuildmat.2018.05.105.
21. Aslani, F., Ma, G., Yim Wan, D. L., Tran Le, V. X. (2018). Experimental investigation into rubber granules and their effects on the fresh and hardened properties of self-compacting concrete. *Journal of Cleaner Production*, 172, 1835–1847. DOI 10.1016/j.jclepro.2017.12.003.

22. Najim, K. B., Hall, M. R. (2012). Mechanical and dynamic properties of self-compacting crumb rubber modified concrete. *Construction and Building Materials*, 27(1), 521–530. DOI 10.1016/j.conbuildmat.2011.07.013.
23. Choi, Y. W., Moon, D. J., Chung, J. S., Cho, S. K. (2005). Effects of waste PET bottles aggregate on the properties of concrete. *Cement and Concrete Research*, 35(4), 776–781. DOI 10.1016/j.cemconres.2004.05.014.
24. Ismail, Z. Z., AL-Hashmi, E. A. (2008). Use of waste plastic in concrete mixture as aggregate replacement. *Waste Management*, 28(11), 2041–2047. DOI 10.1016/j.wasman.2007.08.023.
25. Aswatama, W. K., Suyoso, H. U. N., Tedy, P. (2018). The effect of adding PET (Polyethylen Terephthalate) plastic waste on SCC (self-compacting concrete) to fresh concrete behavior and mechanical characteristics. *Journal of Physics: Conference Series*, 953, 12023. DOI 10.1088/1742-6596/953/1/012023.
26. Afrifah, K. A., Hickok, R. A., Matuana, L. M. (2010). Polybutene as a matrix for wood plastic composites. *Composites Science and Technology*, 70(1), 167–172. DOI 10.1016/j.compscitech.2009.09.019.
27. Bogas, J. A., Gomes, A., Pereira, M. F. C. (2012). Self-compacting lightweight concrete produced with expanded clay aggregate. *Construction and Building Materials*, 35, 1013–1022. DOI 10.1016/j.conbuildmat.2012.04.111.
28. GB175: Common Portland Cement. (2007). (in Chinese). <http://www.jianbiaoku.com/webarbs/book/83154/2286052.shtml>.
29. SL 352: Test Code for Hydraulic Concrete. (2006). (in Chinese). <http://www.jianbiaoku.com/webarbs/book/72375/1515098.shtml>.
30. Craig, P., Wolfe, B. (2012). Another look at the drying of lightweight concrete. *Concrete International*, 53–58. [http://xueshu.baidu.com/usercenter/paper/show?paperid=f87172bc068d0ca4ed47d3771f7552a5&site=xueshu\\_se](http://xueshu.baidu.com/usercenter/paper/show?paperid=f87172bc068d0ca4ed47d3771f7552a5&site=xueshu_se).
31. Tajra, F., Abd Elrahman, M., Lehmann, C., Stephan, D. (2019). Properties of lightweight concrete made with core-shell structured lightweight aggregate. *Construction and Building Materials*, 205, 39–51. DOI 10.1016/j.conbuildmat.2019.01.194.
32. JGJ/T283: Technical Specification for Application of Self-Compacting Concrete. (2012). (in Chinese). <http://www.jianbiaoku.com/webarbs/book/10888/303760.shtml>.
33. Hesami, S., Salehi Hikouei, I., Emadi, S. A. A. (2016). Mechanical behavior of self-compacting concrete pavements incorporating recycled tire rubber crumb and reinforced with polypropylene fiber. *Journal of Cleaner Production*, 133, 228–234. DOI 10.1016/j.jclepro.2016.04.079.
34. Lo, T. Y., Tang, P. W. C., Cui, H. Z., Nadeem, A. (2013). Comparison of workability and mechanical properties of self-compacting lightweight concrete and normal self-compacting concrete. *Materials Research Innovations*, 11(1), 45–50. DOI 10.1179/143307507X196239.
35. Santos, A. C. P., Ortiz-Lozano, J. A., Villegas, N., Aguado, A. (2015). Experimental study about the effects of granular skeleton distribution on the mechanical properties of self-compacting concrete (SCC). *Construction and Building Materials*, 78, 40–49. DOI 10.1016/j.conbuildmat.2015.01.006.
36. Li, H., Huang, F., Xie, Y., Yi, Z., Wang, Z. (2017). Effect of water–powder ratio on shear thickening response of SCC. *Construction and Building Materials*, 131, 585–591. DOI 10.1016/j.conbuildmat.2016.11.061.
37. Ismail, M. K., de Grazia, M. T., Hassan, A. A. A. (2015). Mechanical properties of self-consolidating rubberized concrete with different supplementary cementing materials. *Proceedings of International Conference on Transportation and Civil Engineering, London, March 21-22*, 68–75. DOI 10.17758/UR.U0315331.
38. Aslani, F. (2016). Mechanical properties of waste tire rubber concrete. *Journal of Materials in Civil Engineering*, 28(3), 04015152. DOI 10.1061/(ASCE)MT.1943-5533.0001429.
39. Long, G., Yang, J., Xie, Y. (2017). The mechanical characteristics of steam-cured high strength concrete incorporating with lightweight aggregate. *Construction and Building Materials*, 136, 456–464. DOI 10.1016/j.conbuildmat.2016.12.171.
40. Kovler, K., Jensen, O. M. (2005). Novel techniques for concrete curing. *Concrete International*, 27(9), 39–42.
41. Aslam, M., Shafiq, P., Alizadeh Nomeli, M., Zamin Jumaat, M. (2017). Manufacturing of high-strength lightweight aggregate concrete using blended coarse lightweight aggregates. *Journal of Building Engineering*, 13, 53–62. DOI 10.1016/j.job.2017.07.002.

42. China aggregates association. (2019). Mechanical sand 85 yuan/ton, river sand 130 yuan/ton, the price of sand in Hunan has generally fallen – the price and output of sand aggregate in China in September (in Chinese). <http://www.zgss.org.cn/gongqiuxinxi/2019/9005.html>.
43. China solid waste network. (2019). The project released more than 50 billion yuan, and analyzed the waste incineration market in May from four aspects (in Chinese). <http://www.solidwaste.com.cn/news/297294.html>.
44. Chinese government website. (2013). At present, the disposal cost per ton of garbage in the center of Shanghai is close to 500 yuan (in Chinese). [http://www.gov.cn/jrzq/2013-08/02/content\\_2460243.htm](http://www.gov.cn/jrzq/2013-08/02/content_2460243.htm).
45. Industry observation. (2017). Waste wire tire research. *China Tire Resources Recycling*, (10), 22–23 (in Chinese). [https://kns.cnki.net/kns/brief/default\\_result.aspx](https://kns.cnki.net/kns/brief/default_result.aspx).
46. Qi, X. (2019). Waste rubber utilization transformation focuses on popularizing clean automation. *China Rubber*, 35(04), 37–39 (in Chinese).
47. China industrial information network. (2018). The ceramsite market has generally improved in recent years. In 2017, the size of the ceramsite market rose to 1.308 billion yuan, and the product price rebounded to 155 yuan/m<sup>3</sup> (in Chinese). <http://www.chyxx.com/industry/201811/691898.html>.
48. China waste recovery network. (2019). The domestic PP recycled material recycling price market on October 15th (in Chinese). [http://www.zgfeipin.cn/expo\\_13835\\_1/](http://www.zgfeipin.cn/expo_13835_1/).
49. Qasrawi, H., Asi, I. (2016). Effect of bitumen grade on hot asphalt mixes properties prepared using recycled coarse concrete aggregate. *Construction and Building Materials*, 121, 18–24. DOI 10.1016/j.conbuildmat.2016.05.101.